Chemical Engineering & Processing: Process Intensification 132 (2018) 229–240

Contents lists available at ScienceDirect

Chemical Engineering & Processing: Process Intensification

journal homepage: www.elsevier.com/locate/cep

Monolithic stirrer reactor for vegetable oil hydrogenation: A technical and economic assessment

D.E. Boldrini[a,b,*]

[a] Departamento de Ingeniería Química, Universidad Nacional del Sur (UNS), Avenida Alem 1253, CP 8000, Bahía Blanca, Argentina
[b] Planta Piloto de Ingeniería Química (PLAPIQUI), Universidad Nacional del Sur-CONICET, Camino "La Carrindanga" Km 7, CP 8000, Bahía Blanca, Argentina

ARTICLE INFO

Keywords:
Monolithic stirrer reactor
Vegetable oil hydrogenation
Technical-economic analysis

ABSTRACT

The monolithic stirrer reactor (MSR) which consists on monolithic structures mounted on reactor axis as agitator blades is a novel design with the potential to intensify different production processes. Its most outstanding advantages are the absence of a filtering stage after the reaction and the high-speed mass transfer. In this paper, the technical and economic feasibility of sunflower oil hydrogenation process under MSR ($Pd/Al_2O_3/Al$) configuration was studied considering a 100 ton day^{-1} productive plant, a 20 ton capacity reactor and a final product with 75 iodine index. Moreover, several reaction conditions were taken into account, such as catalyst loading and initial and final reaction temperatures, in order to determine the operating costs. The proposed alternative process could be profitable, displaying a higher Net Present Value (NPV) than the conventional technology one. However, slight variations in the monolithic catalyst cost performed through a sensitivity analysis generate a considerable decrease in NPV, thus determining that the implementation of the proposed alternative technology presents a high economic risk. The achieved results in this study indicate that further research is necessary in order to develop a regenerating procedure to extend the catalyst useful life, thus favouring the monolithic technology economy.

1. Introduction

Vegetable oil hydrogenation is a fundamental process in oleo chemical industry to obtain oils with greater consistency, stability and oxidation resistance than in their natural state. As hydrogenated vegetable oils are renewable and environmentally compatible resources (low eco-toxicity, high biodegradability), they gained greater attention in their use in different industries, such as pharmacy, cosmetics, plastics, detergents, lubricants, fuels, etc. [1–3].

Although the vegetable oil hydrogenation process did not undergo major changes over time, other alternatives have been proposed in order to optimize and develop a more environmentally sustainable industry. In this context, different technologies have been proposed that would enable productive process intensification, or critical inputs use minimization. Fixed-bed or packed-bed reactors are a clear example of this. They can be used continuously and since the catalyst is immobilized no further filtration is required after the reaction [4,5].

Another similar concept to packed-bed reactors are monolithic or structured reactors, which are an attractive alternative over conventional multiphase reactors. Monoliths are formed by a block-shaped ceramic or metallic structure with multiple porous channels in which catalytically active compounds are deposited. The most significant advantages of monoliths are low pressure loss, absence of catalyst separation stage and large granted geometrical surface area [4]. Moreover, monoliths have been studied in several multiphase catalytic applications, especially in reactions restricted by mass transfer [6–12]. Previous studies show that different monolithic reactors configurations to perform vegetable oil hydrogenation have advantages over other technological proposals. For example, their double functionality as catalyst and also stirrer since the monolithic structure is anchored on the reactor axis [4,13,14]. In this regard, structured $Pd/Al_2O_3/Al$ catalyst presented good mechanical stability and was reused over reasonable successive batches [15]. Moreover, taking into account that the active phase is a noble metal, the operating temperature required to perform the reaction is considerably lower; consequently, this energy saving together with the filtering stage elimination could justify the use of the alternative catalyst; thus generating both economic and environmental improvements. Although this reactor/reaction configuration has been studied previously [4,13,14], there are no works related to economic aspects which consider experimental results and the corresponding scaling up in order to reproduce an industrial scale process.

In the present work, different reaction conditions are explored

* Corresponding author at: Departamento de Ingeniería Química, Universidad Nacional del Sur (UNS), Avenida Alem 1253, CP 8000, Bahía Blanca, Argentina.
E-mail address: dboldrini@plapiqui.edu.ar.

https://doi.org/10.1016/j.cep.2018.09.001
Received 27 April 2018; Received in revised form 27 August 2018; Accepted 1 September 2018
Available online 13 September 2018
0255-2701/

Notation

a_L	Gas-liquid interfacial area per unit volume of liquid $[m_{GL}^2\, m_L^{-3}]$
a_S	Liquid-solid interfacial area [m^2]
C	Cis geometric isomer of monoene
C_i	Concentration of component i [kmol m^{-3}]
Cp	Heat capacity [J kg^{-1} K^{-1}]
Cp_i	Heat capacity of the component i [J kg^{-1} K^{-1}]
C_f	Fuel cost [US$ m-3]
C_S	Steam cost [US$ kg^{-1}]
C_y	Cash flow in period y [U$S]
C_0	Initial investment [U$S]
Cτ	Diene having two double bonds in cis-trans position
CC	Diene having two double bonds in cis position
CL	Catalyst load$[kg_{Pd}\, m^{-3}]$
D	Reactor diameter [m]
D_a	Agitador diameter [m]
DFC	Direct fixed costs [U$S]
E_i	Energy interchanged in the equipment i [J]
F_{H_2}	Hydrogen inlet flow,[kmol s^{-1}]
h_W	Water entalpy [kJ kg^{-1}]
h_S	Steam entalpy [kJ kg^{-1}]
IV	Iodine value [dimensionless]
H	Reactor height [m]
HCV	Fuel higher calorific value [MJ m^{-3}]
IRR	Internal rate of return [%]
k_i	Kinetic constant [kmol kg^{-1} s^{-1}]
k_{GL}	Gas-liquid mass transfer coefficient $[m_L^3\, m_{GL}^{-2}\, s^{-1}]$
k_{LS}	Liquid-solid mass transfer coefficient [m s^{-1}]
$K_G = 1/\left(\frac{1}{k_{GL}a_L} + \frac{1}{k_{LS}a_S}\right)$	Total mass transfer resistances [s^{-1}]
m	Heated oil mass [kg h^{-1}]
m_f	Fuel consumption [kg h^{-1}]
m_s	Steam production [kg h^{-1}]
MSR	Monolithic stirred reactor
n	Project life time [years]
N	Stirring rate [rpm]
N_{A0}	Amount of initial moles of compound A [moles]
N_{i0}	Amount of initial moles of compound i [moles]
NPV	Net present value [U$S]
P	Power [kW m^{-3}]
PP	Payback period [years]
Q	Heat exchanged [J h^{-1}]
r	Interest rate [%]
r_{H_2}	H2 reaction rate,$[kmol\, m_{oil}^{-3}\, s^{-1}]$
r_i	Reaction rate of compound i [kmol kg^{-1} s^{-1}]
Re	Reynolds number [dimensionless]
ROI	Return on investment [%]
S	Saturated
t	Time [s]
T	Temperature [K]
T_{BO}	Bleaching oil temperature [K]
T_F	Filtration temperature [K]
T_I	Initial reaction temperature [K]
T_R	Final reaction temperature [K]
T_S	Storage temperature [K]
v	Linear velocity in monolith channels [m s^{-1}]
V	Reactor volume [m^3]
x_A	Conversion of compound A [dimensionless]
y	Project period [year]

Greek letters

ΔH_r	Heat of reaction (Eq. *36*) [J mol^{-1}]
ΔH_r	Heat of reaction (Eqs. *9,21,37*) [J kg^{-1} IV^{-1}]
ΔIV	Iodine value gradient [Adimensional]
ΔT	Temperature gradient [K]
η	Boiler efficiency respect to the HCV [%]
μ	Viscosity [kg m^{-1} s^{-1}]
ρ	Density [kg m^{-3}]
τ	Trans geometric isomer of monoene
ττ	Diene having two double bonds in trans position

under this reactor-catalyst configuration varying both the catalyst load and the initial and final reaction temperatures. Based on the obtained results, a technical-economic balance was developed contrasting traditional process costs with those of the alternative process to determine the feasibility of implementing this technology. Thus, this work will contribute to knowledge related to the application of the MSR in the field of renewable and sustainable chemical industry.

2. Reaction models

The main reactions that take place during the process are the hydrogenation of double bonds and their isomerization from the *cis* to *trans* configuration.

All reactions taking place are shown in Fig. 1.

The kinetics involved in the process, the reaction mechanism and the monolithic stirrer hydrogenation reactor model including the catalyst deactivation phenomenon were obtained from the literature [16].

The reactor was assumed as an ideal semibatch reactor for the gas phase and as a batch reactor for the liquid phase. The general equations that represent the reactor behavior under this configuration are the following:

$$\frac{dC_i}{dt} = r_i \tag{1}$$

$$F_{H_2}(t) = -r_{H_2} V \tag{2}$$

The following statements were considered: heterogeneous model considering the resistances in the gas-liquid/liquid-solid interfaces and the intraparticle diffusional resistance; perfect mixture of reactants and product. All the equations involved in the reactor model were included in Appendix A.

3. Study cases

Two different processes were studied: I) conventional vegetable oil hydrogenation performed in a “Dead End” reactor using commercial Ni catalyst, and II) alternative process using a monolithic stirrer reactor ($Pd/Al_2O_3/Al$). Both technologies were proposed as a semi-continuous process to reproduce an industrial-scale design of the vegetable oil hydrogenation. A 100 ton day^{-1} productive plant and a 20 ton capacity reactor operating at 202.65 kPa gauge were assumed taking into account a typical value from literature [17]. On the other hand,

$$C \xrightarrow{k_1} S\ (r_1) \qquad C \xleftrightarrow{k_{iso}} \tau\ (r_{iso})$$

$$\tau \xrightarrow{k_1} S\ (r_1') \qquad CC \xleftrightarrow{k_{iso}} C\tau\ (r_{iso}')$$

$$CC \xrightarrow{k_2} C\ (r_2) \qquad C\tau \xleftrightarrow{k_{iso}} \tau\tau\ (r_{iso}'')$$

$$C\tau \xrightarrow{k_2} C\ (r_2')$$

$$C\tau \xrightarrow{k_2} \tau\ (r_2'')$$

$$\tau\tau \xrightarrow{k_2} \tau(r_2''')$$

Fig. 1. Reactions involved in vegetable oil hydrogenation process.

degummed, bleached and refined with caustic soda sunflower vegetable oil was considered as raw material and partially hydrogenated oil with a final iodine index (IV) of 75 as final product.

It is should be explained that a "Dead End" is a semi-continuous autoclave reactor in which only the hydrogen necessary to the reaction is introduced in the head space of the hydrogenation vessel without recirculation. Thus, the gas dispersion is performed mainly through mechanical stirrers [18].

3.1. Case I – conventional process

For case I, the conventional process of vegetable oil hydrogenation performed at an industrial scale using a commercial Ni catalyst was analysed. Fig. 2 shows a flow sheet of this process.

Material balance can be represented by the following expression:

$$Mass\ in\ (Raw\ materials) = Mass\ out\ (Wastes + Losses) + Mass\ stored\ (Stored\ materials) \quad (3)$$

where:

$$Raw\ materials = Oil_1 + H_{22} + Catalyst_3 + Bleach\ earth_4 + Citric\ acid_4 \quad (4)$$

$$Wastes = Spent\ bleach\ earth_5 \quad (5)$$

$$Losses = Hydrogen\ losses_6 \quad (6)$$

$$Stored\ materials = Catalyst_7 + Hydrogenated\ oil_8 \quad (7)$$

Sub-index indicates the line in which the material gets in/out.

For each batch, energy balance can be represented by the following expression:

$$Energy\ in\ (E_A + E_B) = Energy\ out\ (E_C + E_B + E_D + E_F) \quad (8)$$

where:

$$E_A = Heat\ delivered\ to\ reach\ the\ reaction\ starting\ temperature\ [m\ Cp\ (T_R - T_{BO})] \quad (9)$$

$$E_B = Heat\ recovered\ in\ the\ oil/oil\ heat\ exchanger\ [m\ Cp\ (T_R - T_F)] \quad (10)$$

$$E_C = Heat\ generated\ by\ the\ exothermic\ reaction\ [\Delta H_r\ m\ \Delta IV] \quad (11)$$

$$E_B = Heat\ delivered\ in\ the\ \frac{oil}{oil}\ heat\ exchanger\ [m\ Cp\ (T_R - T_F)] \quad (12)$$

$$E_D = Energy\ contained\ in\ the\ stored\ product\ [m\ Cp\ (T_F - T_S)] \quad (13)$$

$$E_F = Energy\ lost\ to\ surroundings\ in\ the\ filtering\ stage^* \quad (14)$$

Sub-index indicates the equipment/s in which the energy is exchanged.

The heat of reaction was obtained from the literature ($\Delta H_r = 121\ kJ\ mol^{-1}$) [19].

*Utilities involved in filtering stage correspond to 25% of the process totality [4,20].

The Ni catalyst is generally used agglomerated in high melting point fat (333 K) and flake form. The catalyst amount to be employed depends on the reactor agitation degree and the product type to be obtained. The typical agitation used for the reactor size under study is approximately 120 rpm [17]. A temperature of 423 K (T_R), a 60 min reaction time and about 0.06% w/w of commercial Ni catalyst (25% Ni) respect to the oil to be processed are needed in order to obtain the proposed product (IV = 75) [5].

Approximately 0.883 m^3 (NTP) of H_2 per ton of processed oil is necessary to reduce one unit of iodine value. Considering the H_2 losses during the reactor venting (3–4%), a total H_2 volume of 0.92 m^3 (98% purity) per ton of oil is required [20].

At the beginning of a cycle, which includes the number of batches to be made in a working day, the process begins with the fresh oil heating (T_{BO} = 293 K) until reaching a temperature close to the reaction temperature. Normally, this temperature (T_I) is 423 K when the operating pressure is less than 600 kPa gauge. This step is produced in the measuring tank by heat exchange with service steam. Then, the catalyst is incorporated, vacuum is done and finally hydrogen is injected into the reactor to start the reaction. Once the process started, the mixture is heated by the heat given off by the exothermic reaction until reaching the operating temperature (T_R), which is maintained by circulating cooling fluid through the cooling coil. This recovered energy is then used in another operation, such as storage tanks heating [5].

Once the reaction is completed, the hydrogenated oil is released into the drop tank under reduced pressure. Then, the hydrogenated oil is cooled from the reaction temperature to approximately 393 K in the oil/oil heat exchanger (economizer) before entering next stages, filtering (catalysis filtration) and whitening (safety and polishing filtration). The cooling temperature (T_F) corresponds to the press filters operating temperature.

In this way, it is possible to heat the fresh oil to be hydrogenated in a subsequent batch without supplying steam. Normally, for economy of time sake both the first and the second batch are preheated with service steam.

The most modern economizers can operate with up to 99% efficiency, so the total energy supplied by the oil from the reactor can be transferred to the fresh oil that enters the process [21].

Furthermore, the recovered catalyst in the filters still having activity is reused in new batches. This activity is partially lost because vegetable oil impurities poison it, especially phosphorus and sulphur compounds [5].

3.2. Case II – alternative process (MSR)

In case II, the alternative process of vegetable oil hydrogenation using a monolithic stirrer reactor was analysed. Fig. 3 shows the alternative process flow sheet.

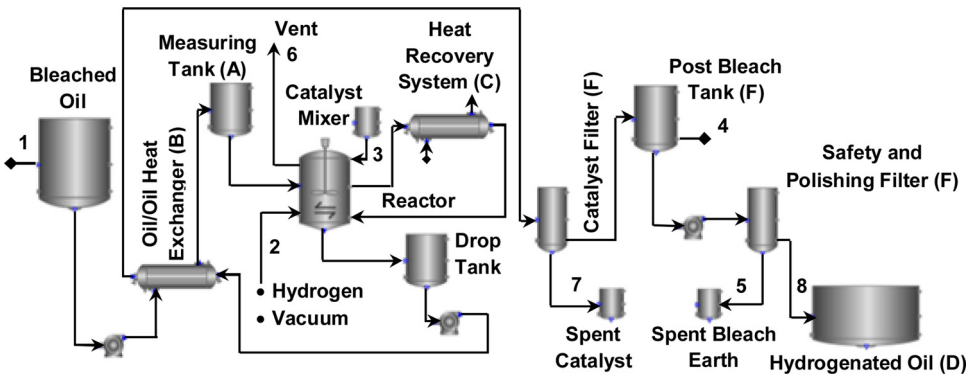

Fig. 2. Case I simplified flow sheet: Conventional process with Ni as catalyst.

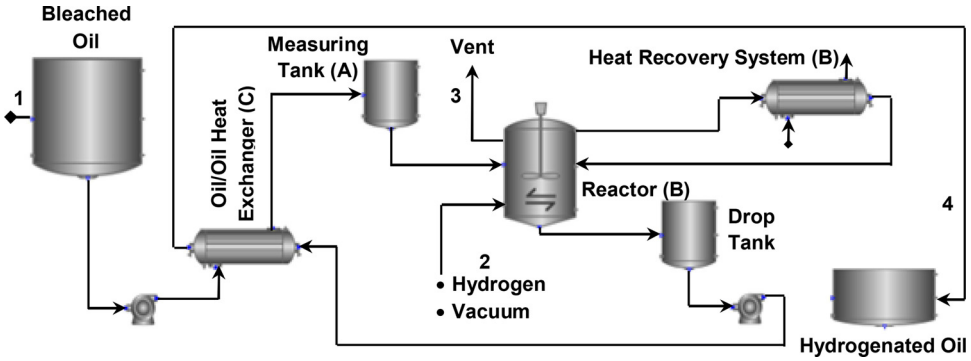

Fig. 3. Case II simplified flow sheet: Alternative process using a monolithic stirrer reactor.

Material balance can be represented by the following expression:

$$Mass\ in\ (Raw\ materials) = Mass\ out\ (Losses) + Mass\ stored\ (Stored\ materials) \quad (15)$$

where:

$$Raw\ materials = Oil_1 + H_{22} \quad (16)$$

$$Losses = Hydrogen\ losses_3 \quad (17)$$

$$Stored\ materials = Hydrogenated\ oil_4 \quad (18)$$

Sub-index indicates the line in which the material gets in/out.

For each batch, energy balance can be represented by the following expression:

$$Energy\ in\ (E_A + E_B + E_2) = Energy\ out\ (E_B + E_C) \quad (19)$$

where:

$$E_A = Heat\ delivered\ to\ reach\ the\ reaction\ starting\ temperature\ [m\ Cp\ (T_I - T_{BO})] \quad (20)$$

$$E_B = Heat\ delivered\ by\ the\ exothermic\ reaction\ to\ reach\ the\ reaction\ temperature\ [m\ Cp\ (T_R - T_I)] \quad (21)$$

$$E_C = Heat\ recovered\ in\ the\ oil/oil\ heat\ exchanger\ [m\ Cp\ (T_R - T_S)] \quad (22)$$

$$E_B = Heat\ generated\ by\ the\ exothermic\ reaction^*\ [\Delta H_r\ m\ \Delta IV] \quad (23)$$

$$E_C = Heat\ delivered\ in\ the\ oil/oil\ heat\ exchanger\ [m\ Cp\ (T_R - T_S)] \quad (24)$$

Sub-index indicates the equipment/s in which the energy is exchanged.

*Discounting the energy considered in E_2.

Analogous to the conventional process, the plant daily operation begins with oil preheating in the measuring tank up to the initial reaction temperature (T_I). For the first two batches, the energy contribution comes from the heat exchange with service steam. From the third batch on, fresh oil is preheated in the oil/oil heat exchanger by heat exchange with the oil coming from the drop tank (previous batch). In the $Pd/Al_2O_3/Al$ structured catalyst case, it was previously reported that no lixiviation takes place during the catalyst lifetime [15] indicating that filtering and bleaching stages are not necessary. Thereby, after the reaction, the oil is cooled to a temperature of 5 K (T_S) above the melting point of the obtained product (311 K) and then diverted to the storage tanks.

4. Cost analysis methods

As described above, the use of a monolithic stirrer reactor involves operating advantages which require considerably less energy than the conventional process. The applicability of these systems is centred on the cost-benefit generated by this technology change [22]. To compare economically the proposed technologies, the operating and investment costs were determined at first and then analysed through economic indicators.

4.1. Fixed capital cost

Acquisition costs (FOB) of the main equipment required in each studied case were taken from literature, considering their characteristic sizes and indexation [23]. FOB cost includes: internals, shells, nozzles, manholes, covers, etc., for each piece equipment; vendor engineering, shop drawings shop testing, certification; shop fabrication labour; typical manuals, small tools, accessories and packaging for shipment by land. FOB cost does not include: owner/contractor indirects; packaging for overseas/air shipment, modularization; freight, insurance, taxes/duties, field setting costs and installation bulks. Other complementary costs associated to the main equipment were also considered following the generic percentages according to the studied process. [24]. Table 1 shows the corresponding costs.

4.2. Operating costs

Hydrogenation is an expensive process, mainly due to reactants -catalyst and hydrogen- and to a lesser extent, energy inputs; hence, one of the key points in vegetable oil modification is the global operating cost because it affects directly the process profitability itself.

Thereby, the analysis of the proposed alternative process application was done considering the following operating costs:

- Raw material cost.
- Catalyst initial cost.
- Catalyst useful life.
- Hydrogen consumption.

Table 1
Complementary costs associated with the production plant facilities.

Complementary costs	Percent (%) of the main equipment purchase cost
Direct costs	
Piping	66
Instrumentation	18
Installation	47
Electrical facilities	11
Building and land	24
Yard improvement	10
Service facilities	70
Indirect costs	
Engineering and construction	74
Other costs	
Contractor's fee and contingency (15% of direct and indirect costs)	39

- Energy consumption in the hydrogenation reactor.
- Filtering stage cost.
- Catalyst recovery after its useful life.
- General expenses.

Based on these parameters and the fixed capital cost, the present technical-economic study was developed considering the scaling up and operation of an industrial scale hydrogenation reactor.

4.2.1. Raw material cost

The raw material cost used in both technologies, 950 U$S ton^{-1}, was estimated according to the current international market [25]. It is important to highlight that transportation cost of raw material was not considered because it was assumed that hydrogenation and vegetable oil refining plants are situated in the same place.

4.2.2. Catalyst initial cost

Machado et al. [22] analysed the economic factors as well as those associated with the process for monolithic reactors in hydrogenation reactions. The authors studied the costs associated to the catalyst, both in its monolithic and conventional (slurry) configuration comparing the advantages and disadvantages of both catalysts systems.

According to the authors, the cost of a catalyst can be estimated pursuant to the following simplified equation:

$$Catalyst\ cost\left[\frac{US\$}{Kg_C}\right] = Manufacturing\ cost\left[\frac{US\$}{Kg_C}\right] + \frac{Metal\ load\ [\%]}{100\%} Metal\ Cost\left[\frac{US\$}{Kg_M}\right] \quad (25)$$

where the metal load is the amount of active metal in the catalyst and the manufacturing costs include the total associated costs, excluding the active metal price.

In this way, the net catalyst cost considering the active metal recovery can be expressed as follows:

$$Net\ catalyst\ cost\left[\frac{US\$}{Kg_C}\right] = Catalyst\ cost\left[\frac{US\$}{Kg_C}\right] + Recovering\ cost\left[\frac{US\$}{Kg_C}\right] - \frac{Recovered\ metal\ [\%]}{100\%} Metal\ cost\left[\frac{US\$}{Kg_M}\right] \quad (26)$$

In the above expression, the recovered metal refers to the amount of active metal recovered per catalyst mass.

Thus, the key to reduce the catalyst contribution to the total process cost is the times it can be reused along with the manufacturing and metal recovering costs.

In order to determine the total catalyst cost, the following items were taken into account:

- Active metal (Pd) = 30,000 US$ kg^{-1} [26].
- Catalytic support = 10,000 US$ hm^{-2} [27].
- Catalyst manufacture = 9 U$S kg^{-1} [28].

The catalyst manufacturing cost contemplates manufacture and raw materials, excluding noble metal and catalytic support. Both the metal dispersion and the other monolithic catalyst characteristics were obtained from literature [16,19].

On the other hand, the current market cost of the fresh nickel commercial catalyst (25% Ni) is 75,000 US$ ton^{-1} while the recovered catalyst cost is 1200 US$ ton^{-1} [20].

4.2.3. Catalyst useful life

Several authors have studied the use of heterogeneous palladium catalysts in vegetable oil hydrogenation [4,15,29]. In all cases, it was determined that although the relative activity declines as the catalyst is reused, the products distribution remains unchanged. This fact corresponds to the carbonaceous compounds formation on the active metal surface [15]. Therefore, as the catalyst is reused and the catalytic surface is covered by the carbonaceous deposits, the activity decays without significant selectivity changes, maintaining an even product distribution.

In the present work, the deactivation model valid for the system under study reported by Boldrini et al. was used [16].

Regarding the useful life of the commercial Ni catalyst used in the conventional process, the catalysts loading is formed by fresh and used fractions according to some pre-established mixing rule although its activity decays considerably during its first use [30]. The amount of catalyst recovered after its useful life is presented in Section 4.2.7.

4.2.4. Hydrogen consumption

As mentioned above, the hydrogen used contributes considerably to the process economy. Analogous to conventional technology, the alternative process requires approximately 0.92 m^3 (NTP) of H_2 in order to reduce one unit of iodine value per ton of oil to be processed. This value is related to the amount of double bonds contained in the oil to be hydrogenated, for each double bound is needed one H_2 molecule. The current cost of hydrogen with purity according to the process requirements is 3 US$ m^{-3} (NPT) [20].

4.2.5. Energy consumption in the hydrogenation reactor

To make a direct comparison between the studied technologies, it is essential to quantify the energetic costs associated to the process and particularly to the hydrogenation reactor. At first, it is necessary to define a reactor operation criterion; that is, the product characteristics reached in each batch (final IV) and the way to manipulate the operative variables; namely, temperature, reaction time and catalyst loading.

As a function of such parameters, the main contributions to the reactor total operating cost without considering the reagents are the following:

- Heat delivered to reach the reaction starting temperature.
- Power supplied to the agitator shaft during the reaction course.
- Heat generated by the exothermic reaction.
- Heat recovered in the temperature drop after the reaction.

4.2.5.1. Costs associated with the heat exchanged in the system. Costs associated with the heat exchanged in the system can be calculated based on fuel consumption used for steam production.

The costs associated with steam generation (C_S) depend on each following contribution: fuel (C_F), raw water supply, boiler feed water treatment, feed water pumping power, combustion air fan, sewer charges for boiler blowdown, ash disposal, environmental emissions control and maintenance materials and labour.

Although the estimation of the steam generation total cost is relatively simple, being this the sum of the all previous contributions, in practice, it is common to use the following approximation [31]:

$$C_S = m_F\, C_F\, (1 + 0.3) \quad (27)$$

0.3 represents a typical value of the contributions sum 2–9 for cases where gas or oil derivatives are used as fuel.

Fuel consumption is directly proportional to the steam production and can be obtained by the following equation:

$$m_F = \frac{m_S\,(H_S - H_W)}{HCV\,\eta} \quad (28)$$

where the term $m_S\,(H_S - H_W)$ represents the delivered heat for steam

generation that will then be exchanged in the process (Eq. (29)).

$$Q = m\,Cp\,\Delta T \tag{29}$$

$$C_p = 4{,}2\,T + 894{,}5 \tag{30}$$

Heat capacity was calculated according to Rojas et al. proposal [32]

For the specific case of natural gas, its higher calorific value (HCV) and boiler efficiency respect to the HCV (η) correspond to 38 MJ m^{-3} and 80%, respectively. The fuel cost (C_F) is 0.14 US$ m^{-3} [33].

Another aspect to consider is the energy recovery through condensate return to the boiler. Steam contains two types of energy: latent and sensitive. When steam is supplied to a given process application, it releases the latent energy to the process fluid and condenses. This condensate retains the sensitive heat the vapour possessed, normally representing 16% of the total energy contained in the vapour.

The condensate contains water and chemical products for the boiler treatment, so its recovery generates greater energy efficiency and a cost reduction in: chemical reagents, replacement water, disposal to the sewer system and environmental regulations compliance.

It is normally estimated that condensates return efficiency is approximately 90% of the total mass of the used steam [34].

4.2.5.2. Costs associated with the power supplied to the agitator shaft and mass transport coefficients scaling up. The power supplied to the agitator is not only important from the point of view of the process economy, but also in the scaling up development because it is directly related to the agitation degree; i.e., with the mass transfer coefficients.

Although there are different criteria to perform a mechanically agitated reactor scaling up, the most used in this type of systems is the constant power-volume ratio [35]. It requires that the term $N^3 D_a^5$ remains constant to obtain equal values of the gas-liquid mass transport coefficient ($k_{GL}a_L$) during scaling up [36]. Although this criterion is reasonable and has been used to a large extent, it only applies to similarly configured reactors.

Chen et al. [17] developed a technique for $k_{GL}a_L$ estimate in vegetable oil hydrogenation reactors as an empirical correlation function of the following intensive parameters: P/V, H/D y Re. Since this correlation was developed from 5 reactors with capacities in the range of 0.1–29,100 kg with dissimilar designs, it could be used in the scaling up and simulation of industrial equipment with different geometrical characteristics and configurations. Eq. 31 details the model mentioned above:

$$k_{GL}a_L = 0.5208 + 5.206^{-6}Re + 4.055^{-5}P/V - 1.699H/D - 1.092^{-9}ReP/V - 5.221^{-12}Re^2 + 8.064^{-11}(P/V)^2 + 0.4826(H/D)^2 \tag{31}$$

where:

$$Re = \frac{D_a^2\,N\,\rho}{60\,\mu} \tag{32}$$

$$\rho = 931 - 0.64145(T - 273K) \tag{33}$$

$$\mu = 0.0001\,exp\left(\frac{958.6}{T-144}\right) \tag{34}$$

Density and viscosity were calculated according to literature proposals [37,38]. The value predicted by this equation and the one obtained experimentally for a laboratory scale MSR were compared to validate the previous expression for monolithic stirrer reactor case. Sánchez M [39]. determined that the gas-liquid mass transfer coefficient ($k_{GL}a_L$) value is 0.15 s^{-1} for the same system used in the development of the model employed in this work (Reactor Parr® model 4560 with control of agitation and temperature model 4842).

The power value was experimentally determined from the current and operating voltage values of the reactor studied. The characteristic parameters of the used system are shown in Table 2.

On the other hand, the solid-liquid mass transfer coefficient ($k_{LS}a_S$) was calculated from the Sherwood number correlation proposed by Hoek and valid for a three-phase system with monolithic stirrer. For the correlation determination, the fluid velocity inside the monolith channels, which mainly depends on stirring speed, operating temperature and monolith cell density, has to be known. Varying the cells density (100–400 cpsi), the speed increases considerably (4 times) [40]; conversely, the monolith length does not affect the speed inside the channels.

Furthermore, Boldrini et al. [41] determined the speed inside the channels in a monolithic system geometrically like that presented in this paper as a function of the temperature and agitation degree. Considering these results and the relationship between the speed inside the channels and the monoliths cell density, a correlation was obtained using the statistical software STATGRAPHICS Centurion Version XV.2 (Statpoint Technologies Inc.).

The electric consumption of the impeller was calculated according to a typical power value considering the reactor type and capacity (2 kW m^{-3}) and the electricity current cost for an industrial installation (0.1 US$ kWh^{-1}) [42,43]. Based on this value, the gas-liquid mass transport coefficient ($k_{GL}a_L$) was calculated for the industrial scale MSR using Eq. (31). The constructive parameters of the proposed production reactor are detailed in Table 2.

4.2.6. Costs associated with the filtering stage

As mentioned above, the conventional process of vegetable oil hydrogenation requires a filtration step to remove the catalyst particles and a whitening step to remove the remaining traces of nickel leached from the catalyst. Table 3 details the operating costs associated with the filtering process related to the amount of raw material to be processed.

According to Boger et al. [4], this stage contribution to the global process economy represents 20% of the total operating costs.

Considering that a filtering/bleaching stage is not necessary, the generated economic and environmental savings would favour the alternative technology implementation.

4.2.7. Catalyst recovery after its useful life

The recovered catalyst in the conventional process possesses is circa 8% Ni; hence, it would be necessary to use 0.18% catalyst respect to the oil mass to be processed when using recovered catalyst. This fact corroborates the importance that the catalyst recovery has on the process economy.

For monolithic catalysts, the amount of active metal recovered after the catalyst lifetime is around 95–99% [22]. This fact is in agreement with experimental results previously reported in which the amount of noble metal deposited on the monolith remains unchanged although the catalyst is progressively deactivated until losing all its activity because of active metal surface covering by carbonaceous residues [15]. In this work, 97% metal recovery and a metal recovery cost of around 740 U$S kg_{Pd}^{-1} were considered [44].

Table 2
Characteristic parameters of the laboratory and industrial scale reactors.

Parameter	Hydrogenator scale	
	Laboratory	Industrial
Size [kg]	0.22	20,000
Reactor height (H), [m]	0.08	4.5
Reactor diameter (D), [m]	0.063	2.55
Agitator diameter (D_a), [m]	0.06	0.56
Reactor volume (V), [m^3]	0.00025	23
Temperature (T), [K]	373	333-413
Agitation degree (N), [rpm]	1400[a]	120
Baffles	No	Yes
Type of agitator	Monolithic (400 cpsi)	Monolithic (100 cpsi)
No. of agitators	1	3

[a] Experimentally determined with a digital tachometer Schwyz SC114.

Table 3
Filtering stage operative costs [20].

	Cost	Consumption	Operative cost [U$S ton^{-1}]
Citric acid	1.75 U$S kg^{-1}	0.5 kg ton^{-1}	0.88
Bleach earth	0.6 U$S kg^{-1}	1 kg ton^{-1}	0.60
Oil lost	1.08 U$S kg^{-1}	1 kg ton^{-1}	1.10
Earth eviction	0.17 U$S kg^{-1}	1 kg ton^{-1}	0.17
Filtering clothes	4 U$S cloth^{-1}	1 cloth p/30 ton	0.13
Services[a]	–	–	9.80
Total	–	–	12.7

[a] It includes electricity, steam, water, air and nitrogen.

Another aspect to consider is the substrate recovery. Anodized aluminium synthesis is known to comprise a series of relatively complex stages, requiring substantial material, energy or human resources [45].

It has already been reported that monolithic anodized aluminium substrate possesses good mechanical stability and its morphological properties can be recovered after an adequate cleaning treatment [15].

Furthermore, Boldrini [46] determined that it is possible to reuse the substrate after catalyst deactivation if it is cleaned and re-impregnated with the active metal, which provides a new variant to optimizing costs associated with the use of this technology. Metal recovery could be performed after a series of deactivation-recovery-impregnation cycles, thus prolonging the substrate useful life. In this work, it was considered that the substrate can be reused only once according to the experimental results reported.

4.2.8. General expenses

Services, maintenance/labour, chemical reagents and others are included in the general expenses and were calculated according to the plants operational capacity [20]. For both technologies, the expenses related to maintenance/labour and reagents correspond to 7.38 and 0.41 U$S ton^{-1}, respectively; services correspond to 3.2 U$S ton^{-1} and those catalogued as “others” were calculated as 5% of the total operating costs.

4.3. Economic indicators

To compute each proposed scenario economy, a 15 years life time project with 1 year for plant construction and start-up, and constant equipment depreciation during the project useful life were considered. It was assumed that the processing plant works 330 days per year operating at 100% of its capacity at all times. Funding comes from private investments and no loan has been considered. Comparison between both technologies was performed considering various economic indicators: Net Present Value (*NPV*), Return on Investment (*ROI*), Internal Rate of Return (*IRR*) and Payback Period (*PP*). An interest rate of 15% and a product cost of 1260 US$ ton^{-1} was considered according to the current international market. Below it shown the equations for the economic indicators calculation:

$$NPV = \sum_{y=1}^{n} \frac{C_y}{(1+r)^y} - C_0 \quad (35)$$

Table 5
Equipment costs.

Equipment	Main characteristics	Costs [U$S]	
		Case I	Case II
Reactor	20 ton/batch reactor[a]	340,000	340,000
Heat exchangers (2)	Fixed-tube[a,b]	40,000	40,000
Measuring tank	20 ton/batch cylindrical tank[a]	10,000	15,000
Drop tank	20 ton/batch mixer[a]	15,000	15,000
Catalyst mixer	0.1 m^3 mixer[a]	4000	N/R
Oil transfer pumps (3)	Centrifugal type, cast steel, 30 m^3/h	6000	6000
Filter press pumps (2)	Centrifugal type, cast steel, 30 m^3/h	6000	N/R
Post bleach tank	20 ton/batch mixer[a]	15,000	N/R
Catalyst filter	Vertical filter, 0.75 m^3[a]	90,000	N/R
Safety and polishing filter	Vertical filter, 0.75 m^3[a]	90,000	N/R
Spent catalyst tank	Cylindrical tank, 0.75 m^3	4000	N/R
Spent bleach earth tank	Cylindrical tank, 0.75 m^3	4000	N/R
Hard oil tank (4)	25 m^3[a]	50,000	50,000
Total		674,000	466,000

[a] Material of construction: carbon steel.
[b] Considering a typical overall heat transfer coefficient value (U = 100 W m^{-2} K^{-1}) [48].

Table 6
Summary of fixed costs associated with each technology.

	Fixed costs [U$S]	
	Case I	Case II
Total capital investment	3,557,709	2,459,781
Equipment purchase cost	674,000	466,000
Direct fixed capital (DFC)	3,093,660	2,138,940
Working capital[a]	464,049	320,841

[a] Calculated as 15% of the DFC [24].

Table 4
Different simulated reaction conditions.

Cycle [#]	T_I [K]	T_R [K]	CLx10^{-2} [kg m^{-3}][a]	Cycle [#]	T_I [K]	T_R [K]	CLx10^{-2} [kg m^{-3}][a]	Cycle [#]	T_I [K]	T_R [K]	CLx10^{-2} [kg m^{-3}][a]
1–5	333	333	3.2–5.0	76–80	343	403	3.2–5.0	151–155	373	373	3.2–5.0
6–10	333	343	3.2–5.0	81–85	343	413	3.2–5.0	156–160	373	383	3.2–5.0
11–15	333	353	3.2–5.0	86–90	353	353	3.2–5.0	161–165	373	393	3.2–5.0
16–20	333	363	3.2–5.0	91–95	353	363	3.2–5.0	166–170	373	403	3.2–5.0
21–25	333	373	3.2–5.0	96–100	353	373	3.2–5.0	171–175	373	413	3.2–5.0
26–30	333	383	3.2–5.0	101–105	353	383	3.2–5.0	176–180	383	383	3.2–5.0
31–35	333	393	3.2–5.0	106–110	353	393	3.2–5.0	181–185	383	393	3.2–5.0
36–40	333	403	3.2–5.0	111–115	353	403	3.2–5.0	186–190	383	403	3.2–5.0
41–45	333	413	3.2–5.0	116–120	353	413	3.2–5.0	191–195	383	413	3.2–5.0
46–50	343	343	3.2–5.0	121–125	363	363	3.2–5.0	196–200	393	393	3.2–5.0
51–55	343	353	3.2–5.0	126–130	363	373	3.2–5.0	201–205	393	403	3.2–5.0
56–60	343	363	3.2–5.0	131–135	363	383	3.2–5.0	206–210	393	413	3.2–5.0
61–65	343	373	3.2–5.0	136–140	363	393	3.2–5.0	211–215	403	403	3.2–5.0
66–70	343	383	3.2–5.0	141–145	363	403	3.2–5.0	216–220	403	413	3.2–5.0
71–75	343	393	3.2–5.0	146–150	363	413	3.2–5.0	221–225	413	413	3.2–5.0

[a] CL was varied from the following values: 0.032, 0.037, 0.042, 0.047 and 0.05 kg m^{-3}. Kg refers to the Pd exposed mass.

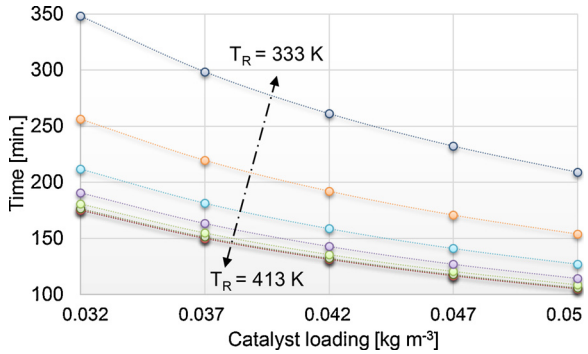

Fig. 4. Total times associated with the cycles performed at an initial temperature of 333 K.

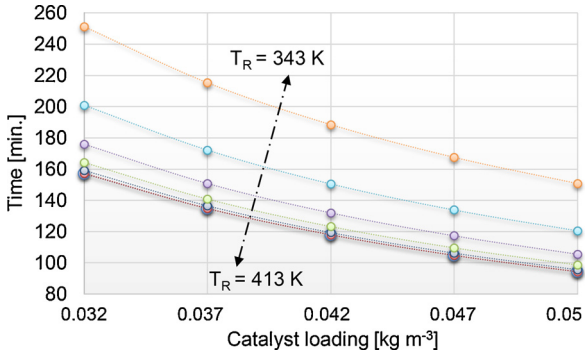

Fig. 5. Total times associated with the cycles performed at an initial temperature of 343 K.

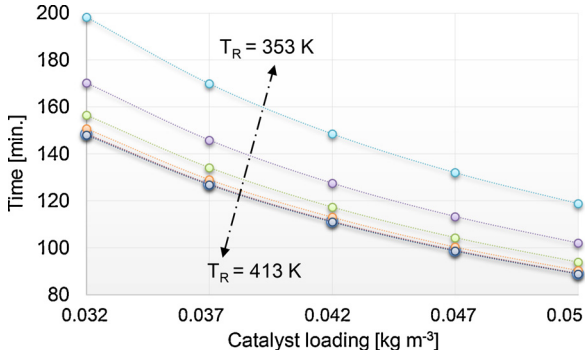

Fig. 6. Total times associated with the cycles performed at an initial temperature of 353 K.

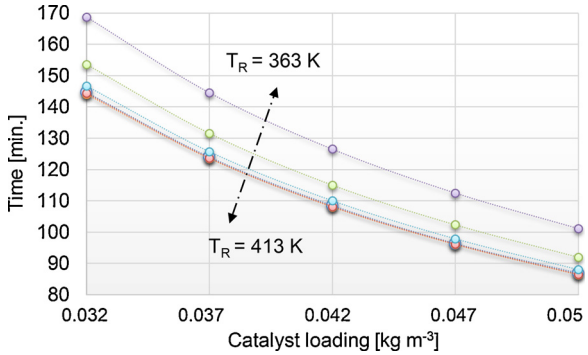

Fig. 7. Total times associated with the cycles performed at an initial temperature of 363 K.

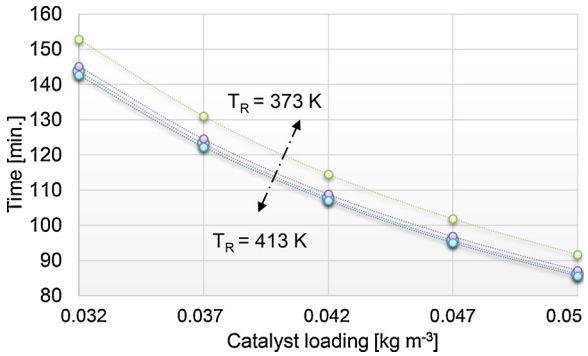

Fig. 8. Total times associated with the cycles performed at an initial temperature of 373 K.

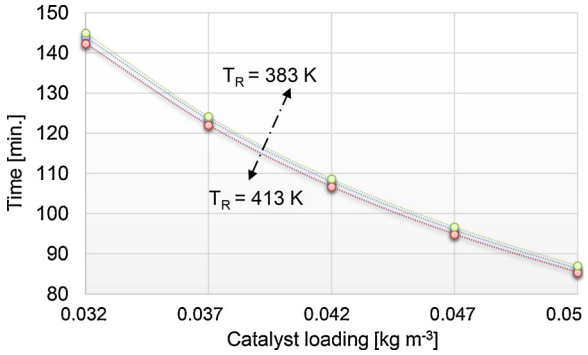

Fig. 9. Total times associated with the cycles performed at an initial temperature of 383 K.

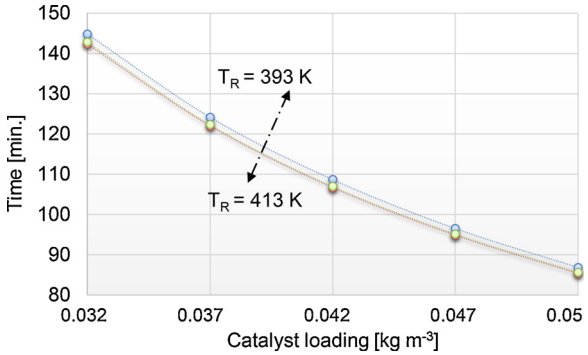

Fig. 10. Total times associated with the cycles performed at an initial temperature of 393 K.

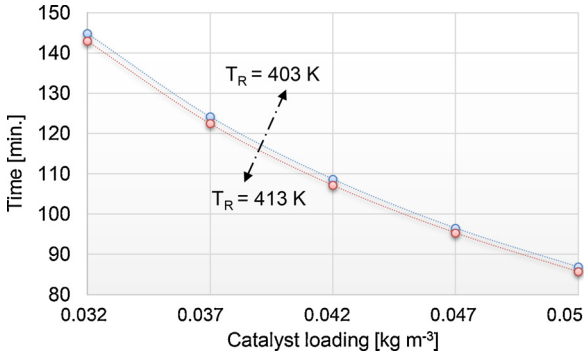

Fig. 11. Total times associated with the cycles performed at an initial temperature of 403 K.

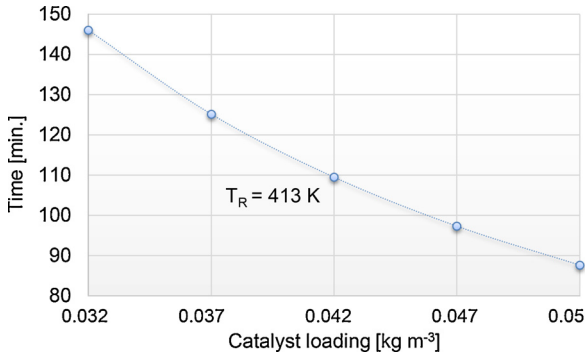

Fig. 12. Total times associated with the cycles performed at an initial temperature of 413 K.

Table 7
Operating costs corresponding to each technology.

	Operating costs [U$S year^{-1}]	
	Case I	Case II
Catalyst cost[a]	1,461,240	2,077,733
Hydrogen consumption	5,063,850	5,063,850
Electric consumption	35,950	17,490
Steam consumption	24,697	7,742
Filtering stage	407,060	–
Services	106,115	44,507
General expenses	1,928,180	1,924,804
Raw material	26,070,000	26,070,000
Total operating costs	35,097,092	35,206,126

[a] Includes recovery cost.

Table 8
Economic indicators.

	Case I	Case II
Product profit [U$S year^{-1}]	41,580,000	41,580,000
ROI [%]	26.4	32.6
NPV [U$S]	2,379,049	2,409,320
IRR [%]	25.8	30.2
PP [years]	3.3	2.6
Interest rate [%]	15	15

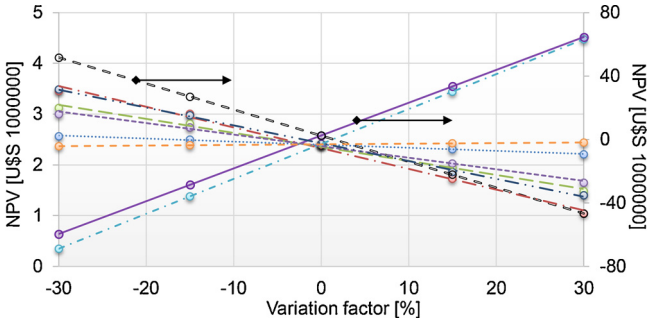

Fig. 13. NPV sensitivity analysis of the vegetable oil hydrogenation process. Ref.: (.. .) support cost, (-˙-) manufacturing cost, (- - -) Pd cost, (- - -) Pd recovering cost, (- · -) recovered Pd percentage, (- - -) global mass transport coefficient, (-˙·-˙-) interest rate, (-) product selling price, (=) raw material cost.

$$ROI = \frac{\left(\sum_{y=1}^{n} C_t\right) - C_0}{C_0} \tag{36}$$

$$PP = \frac{C_0}{\left(\left(\sum_{y=1}^{n} C_y\right)/n\right)} \tag{37}$$

where: C_y is the cash flow on period y, n the project life time, r the interest rate and C_0 the initial investment.

IRR corresponds to the value of r that generate a *NPV* equal to zero.

4.4. Sensitivity analysis

In order to investigate the effects of the uncertainty associated to certain variables that determine the cash flow on the alternative technology economic viability, a sensitivity analysis was performed. It took into account the following factors: interest rate, global mass transfer coefficient (K_G), support cost, catalyst manufacturing cost, palladium price, noble metal recovery cost, product selling price, raw material cost and recovered Pd percentage. Relative variations in the range of -30% to +30% with 15% increase each time were taken into account except for the recovered metal percentage where variations of 0.1% each time were considered.

5. Process simulation and optimization

Simulation and optimization were done using the advanced modelling software GProms (Process Systems Enterprise Ltd.) under academic license.

A monolithic stirrer reactor model presented previously was used [16], adapting it to the industrial scale operating conditions. Simulation was done varying both the catalyst load and the initial and final reaction temperatures while the optimal operation corresponds to that minimize the operating costs. To perform the simulation, all algebraic and differential equations involved in the reactor model (Appendix A) were solved simultaneously over time to achieve a final product with IV = 75. The initial conditions were determined by the raw material composition.

Given that the original mathematical model only contemplated an isothermal operation contrary to the industrial process, the energy balance corresponding to a discontinuous stirred tank reactor (TAD) operating adiabatically was added. This can be described by the following expression [47]:

$$T_f = T_0 - \frac{N_{A0}\,\Delta H_r\,(T_f)\,x_A}{\sum_1^n N_{i0}\,Cp_i} \tag{38}$$

Considering that there is only one reagent and expressing the heat of reaction in units of J kg^{-1} IV^{-1}, the above equation can be expressed as:

$$T = T_0 - \frac{\Delta H_r\,(T)\,\Delta IV}{C_p} \tag{39}$$

Regarding the relation $-\Delta H_r/C_p$ this can be approximated to 1.7 K IV^{-1} [5].

It should be noted that the mathematical model was developed to reproduce the initial temperature increase and the isothermal operation after reaching the desired reaction temperature in the required cases, whereas the isothermal mode operation was also considered.

The sum of all operating costs involved was considered as an objective function to be minimized in order to optimize economically the process.

5.1. Operating limitations

The aim of this work is to model the vegetable oil hydrogenation reactor in order to obtain process conditions that minimize operating costs to compare them with the traditional process.

Since in the real operation some involved parameters cannot exceed certain values because of equipment design or process restrictions, it is necessary to define the limits between which the control variables must be maintained during the reactor modelling.

Mainly, the time of each daily production cycle must have a

maximum duration in order to respect the logistics and economy of time of conventional operations. For a product with IV = 75, the operating time for 5 batches per day is 300 min. [20].

On the other hand, heat extraction capacity of the conventional system must be taken into account. Although it is hypothetically possible to operate with relative high catalyst loadings and high reaction temperatures, the fact that current industrial reactors can operate with maximum variations in the order of 3 IV $min.^{-1}$ must be considered. Hence, the minimum operating time for a product with IV = 75 should be approximately 14 min per batch.

An experimental design considering these requirements was developed. For all cases in which reaction times were less than 14 min, the reactor simulation was performed by reducing the agitation degree; i.e., decreasing the rpm and thus the mass transport coefficients value so that the end reaction time equals 14 min. On the other hand, all those scenarios where the operating time exceeded 300 min were discarded from the technical-economic analysis.

5.2. Experimental design

To evaluate the trends and times associated with each operation, the reactor was modelled by varying the catalyst loading (CL) and the initial (T_I) and final (T_R) reaction temperature. A total of 225 cycles were simulated, in which each cycle contemplates 5 batches of 20,000 kg of oil to be processed, totalling 100 ton day^{-1} production as previously stated. Table 4 shows the different operation conditions simulated.

6. Results and discussion

Table 5 shows the main equipment investment costs for both studied technologies.

Equipment costs associated with the reaction stage are equivalent for both study cases; however, filtering stage equipment for case I must be considered separately since equipment investment cost for case II is 30% less than conventional technology.

Table 6 shows the total fixed costs associated with each technology studied.

The total investment cost as well as the main equipment is 30% lower in case II because the factor applied to the main equipment cost to quantify the working capital and auxiliary facilities is equivalent for both technologies. For case I fixed costs, the total capital investment is similar to the values reported by Kellens et al. (De Smet) [20].

In order to define the applicability of the model proposed by Chen et al. [17] (Eq. (31)) to an MSR, the power related to the laboratory scale reactor detailed in Table 2 was determined experimentally. The current, voltage and power found were: 0.12 A, 69 V and 8.2 W, respectively. The Reynolds number 11,450 was obtained, thus determining an $k_{GL}a_L$ equal to 0.17 s^{-1}. This value yields an error of 13% respect to that found experimentally by Sánchez M. [39], indicating that the proposed model can be used in order to scale up the MSR. Mass transport coefficient ($k_{GL}a_L$) for the industrial scale MSR was determined from Eq. (31), while the liquid-solid mass transport coefficient ($k_{LS}a_S$) was determined according to the Hoek proposal [40]. Eq. (40) shows the obtained correlation (R-squared = 98.13%) to determine the fluid velocity inside the monoliths channels:

$$v = 1.56054 - 0.00814131\,N - 0.00375655\,T + 0.00000119583\,N^2 + 0.0000225901\,N\,T \quad (40)$$

Both mass transfer coefficients were introduced into the reactor mathematical model, considering the operational variables for its calculation. The obtained values reflected the high speed mass transfer offered by the monolithic catalyst because of the higher flow through the monolith channels and the improved gas–liquid mass transfer [49].

Figs. 4–12 show the operating times obtained for the different reaction conditions proposed in Table 4.

Figs. 4–12 show that the operating times associated with each cycle decrease as the final temperature or catalyst loading increases as expected because reaction rate depends on these parameters. Given that cycle 1 (Fig. 4) exceeds 300 min of operation, it was discarded from the analysis.

When a maximum temperature of 383 K is exceeded, the total operating time of each cycle does not change considerably for any operations implemented, indicating that the reaction enters the diffusional control zone above this temperature.

Through the optimization performed on the different simulated reaction conditions associated with monolithic technology (Table 4), it was determined that operating costs are minimized in cycle 221 (T_I = 413 K, T_R = 413 K, CL = 0.032 kg m^{-3}). It should be noted that although the lowest value found corresponds to this cycle, all cycles with this same CL and maximum temperatures of 383 K differ very little from this result. As previously mentioned, the reaction would begin to operate under diffusional regime above this maximum temperature. Hence, when increasing CL (constant T_I and T_R), the operation times decrease a little showing no appreciable energy saving. Catalyst cost contribution is more significant than energy costs (Table 7), so the operating costs are penalized with the catalyst loading increase under these conditions.

On the other hand, the operation at higher temperatures generates a decrease in reaction time due to the exponential increase in reaction rate. Although steam consumption is greater, it increases linearly with temperature increase, while electricity consumption decreases exponentially. The relationship between costs associated with electricity consumption and steam generation causes operating cost to fall.

Table 7 details operating costs associated to both studied cases. Case II operating cost is slightly higher than the conventional technology case (< 1%). Although energy consumption -electricity, steam, services- is 58% lower for the MSR, mainly because of palladium high activity in relation to Ni, the monolithic catalyst cost threatens the alternative technology economy. Hence, this factor is determinant in case II operating costs even though this process is economically favoured by the filtering stage elimination.

Table 8 reports the economic indicators calculated in order to compare both technologies.

According to the economic indicators, the alternative technology (case II) appears as the most profitable, presenting higher NPV (10% interest rate), ROI and IRR. On the other hand, payback period is less. NPV is higher in case II even when operating costs are higher because the alternative technology investment costs are lower. This indicates that for existing production plants where it would not be necessary to invest in equipment the technology change would be less profitable. Regarding the value of IRR, this is comfortably higher than the interest rate indicating that the project would be feasible to be performed without running into any risks. ROI found shows the gain obtained in relation to the capital invested is acceptable.

As mentioned above, the catalyst cost has considerable heft in case II operating costs. Therefore, the effect of the costs related to the monolithic catalyst as well as the interest rate, global mass transfer coefficient (K_G), product selling price and raw material cost were analysed. Fig. 13 presents the results of the performed sensitivity analysis.

Recovered palladium amount is the most determining factor in the NPV when sensitive changes are made. It can be seen that less than 94% recovery would lead to negative NPV. Changes in interest rate and manufacture costs, palladium and noble metal recovery are less influential, but nonetheless important. Overall mass transfer coefficient and catalytic support cost are not very determining.

These results are attributed mainly to higher palladium cost in comparison to the other monolithic catalyst manufacturing components, even though palladium is added in small proportion. When the noble metal recovery is not effective enough, its loss is very important in the process economy. On the other hand, when palladium market

price changes, the effect is not as noticeable as it affects both the purchase and Pd recovery in the same way.

Although the changes in global mass transfer coefficient generate a modification in operating times, the costs associated with energy contribution dependent on the operating time are not determining in the total operating cost.

Besides, NPV falls below case I NPV by increasing interest rate, manufacturing costs, palladium and noble metal recovering, or decreasing the recovered palladium amount; thus evidencing that the alternative technology becomes less profitable than conventional technology before small perturbations in catalyst cost.

Variations on the product selling price and the raw material cost have been done in order to represent how changes in the market might affect case II process economics. Fig. 13 shows that both product selling price and raw material cost affect the NPV process considerably because of the plant productive capacity. Variations greater than -2% in the product selling price, or lesser than +5% in the raw material cost lead to a negative NPV, indicating a high sensibility to these variables.

Based on these results, it can be affirmed that the implementation of a monolithic stirrer reactor in the vegetable oil hydrogenation process could be feasible, but it presents a high economic risk.

7. Conclusions

Through the technical-economic study performed, it was possible to establish the trend in the reaction conditions employed to reduce the operating costs in the vegetable oil hydrogenation through the implementation of a monolithic stirrer reactor in the production process. It was determined that the operating cost is minimized when operating with small catalyst loadings and high initial and final reaction temperatures.

Besides, the proposed alternative process can be profitable with higher NPV than that of the conventional technology even though the operating costs are higher for the monolithic technology.

The sensitivity analysis determined that the process profitability is heavily influenced by the catalyst cost, particularly with the noble metal recovery percentage, even to the extent of reaching negative NPV.

Slight changes in the catalyst cost make the alternative technology NPV less appealing than that of conventional technology, thus determining that the MSR implementation carries a considerable economic risk. This indicates the need for future research in order to develop a regenerating procedure to extend the catalyst useful life.

Acknowledgments

The author thanks Prof. Dr. Daniel E. Damiani for many helpful discussions. This research was supported by the National Scientific and Technical Research Council (CONICET) and Universidad Nacional del Sur (UNS), Argentina.

Appendix A. Supplementary data

Supplementary material related to this article can be found, in the online version, at doi: https://doi.org/10.1016/j.cep.2018.09.001.

References

[1] B. Nohair, C. Especel, G. Lafaye, P. Marécot, L.C. Hoang, J. Barbier, Palladium supported catalysts for the selective hydrogenation of sunflower oil, J. Mol. Catal. A: Chem. 229 (1) (2005) 117–126.
[2] C.D. Alexandrino, S.M. Morais, M.S. Oliveira, L.K. Machado, C.G. Martins, A.A. Craveiro, N.C. Rocha, C.P. Valle, J.Q. Malveira, F.A. Jorge, Influence of hydrogenation and antioxidants on the stability of soybean oil biodiesels, Eur. J. Lipid Sci. Technol. 115 (6) (2013) 709–715.
[3] J.J. Burdeniuc, J.D. Toblas, R.J. Keller, Y.M. Jeon, Additives For Improving Natural Oil Based Polyurethane Foam Performance. U.S. Patent 13,534,171, June 27, 2012.
[4] T. Boger, M.M. Zieverink, M.T. Kreutzer, F. Kapteijn, J.A. Moulijn, W.P. Addiego, Monolithic catalysts as an alternative to slurry systems: hydrogenation of edible oil, Ind. Eng. Chem. Res. 43 (10) (2004) 2337–2344.
[5] W. Hamm, R.J. Hamilton, G. Calliauw, Edible Oil Processing, second edition, John Wiley & Sons, Ltd., Hoboken, NJ, 2013, pp. 164–166.
[6] A. Cybulski, J.A. Moulijn, Monoliths in heterogeneous catalysis, Catal. Rev. Sci. Eng. 36 (2) (1994) 179–270.
[7] F. Kapteijn, T.A. Nijhuis, J.J. Heiszwolf, J.A. Moulijn, New non-traditional multiphase catalytic reactors based on monolithic structures, Catal. Today 66 (2) (2001) 133–144.
[8] D.I. Enache, P. Landon, C.M. Lok, S.D. Pollington, E.H. Stitt, Direct comparison of a trickle bed and a monolith for hydrogenation of pyrolysis gasoline, Ind. Eng. Chem. Res. 44 (25) (2005) 9431–9439.
[9] R.E. Albers, M. Nyström, M. Siverström, A. Sellin, A.C. Dellve, U. Andersson, W. Herrmann, T. Berglin, Development of a monolith-based process for H_2O_2 production: from idea to large-scale implementation, Catal. Today 69 (1) (2001) 247–252.
[10] R. M. Machado, D. J. Parrillo, R. P. Boehme, R. R. Broekhuis, Use of a monolith catalyst for the hydrogenation of dinitrotoluene to toluenediamine. U.S. Patent 6, 005,143, A, December 21, 1999.
[11] A.G. Bussard, Y.G. Waghmare, K.M. Dooley, F.C. Knopf, Hydrogenation of α-methylstyrene in a piston-oscillating monolith reactor, Ind. Eng. Chem. Res. 47 (14) (2008) 4623–4631.
[12] Y.G. Waghmare, A.G. Bussard, R.V. Forest, F.C. Knopf, K.M. Dooley, Partial hydrogenation of soybean oil in a piston oscillating monolith reactor, Ind. Eng. Chem. Res. 49 (14) (2010) 6323–6331.
[13] A.J. Bird, T.M. Priestley, J.M. Winterbottom, Process for the hydrogenation of a vegetable oil. U.S. Patent 4,163,750, August 07, 1977.
[14] R.C. Cornelison, W. R. Alcorn, Process for hydrogenation of organic compounds. European Patent 0,233,642,A2, August 26, 1987.
[15] D.E. Boldrini, G.M. Tonetto, D.E. Damiani, Experimental study of the deactivation of Pd on anodized aluminum monoliths during the partial hydrogenation of vegetable oil, Chem. Eng. J. 270 (2015) 378–384.
[16] D.E. Boldrini, D.E. Damiani, G.M. Tonetto, Mathematical modeling of the partial hydrogenation of vegetable oil in a monolithic stirrer reactor, AIChE J. 60 (10) (2014) 3524–3533.
[17] A.H. Chen, D.D. McIntire, P. Gibson, J.E. Covey, Investigation and modeling of mass transfer in soybean oil hydrogenators, J. Am. Oil Chem. Soc. 60 (7) (1983) 1326–1330.
[18] M. Bockisch, Fats and Oils Handbook, AOCS Press, Champaign, IL, 1993, pp. 545–612.
[19] M.J.F. Sánchez, D.E. Boldrini, G.M. Tonetto, D.E. Damiani, Palladium catalyst on anodized aluminum monoliths for the partial hydrogenation of vegetable oil, Chem. Eng. J. 167 (2011) 355–361.
[20] M. Kellens, M. Hendrix, J. Melo, Desarrollos en la modificación de grasas: hidrogenación-interesterificación-fraccionamiento. Características y beneficios, Parte 1. *A&G* 32 (1998) 399–411.
[21] M.J. Kokken, Hydrogenation, Energy Recovery and Automation, Proceedings of World Conference on Emerging Technologies in the Fats & Oils Industry (1986).
[22] R.M. Machado, R.R. Broekhuis, A.F. Nordquist, B.P. Roy, S.R. Carney, Applying monolith reactors for hydrogenations in the production of specialty chemicals-process and economic considerations, Catal. Today 105 (3) (2005) 305–317.
[23] M.S. Peters, K.D. Timmerhaus, R.E. West, Plant Design and Economics for Chemical Engineers, fifht edition, McGraw-Hill, New York, NY, 2003 Equipment Costs File.
[24] M.S. Peters, K.D. Timmerhaus, Plant Design and Economics for Chemical Engineers, fourth edition, McGraw-Hill, Singapore, 1991, pp. 150–215.
[25] International Monetary Fund (IMF) Home Page-Primary Commodity Prices. http://www.imf.org/external/np/res/commod/index.aspx (Accessed 14 January 2018).
[26] National Association of Securities Dealers Automated Quotation (NASDAQ) Home Page-Palladium. http://www.nasdaq.com/markets/palladium.aspx (Accessed 20 December 2017).
[27] Yogoon Tech Home Page-Anodized Aluminum Sheet. http://www.yogoon.com/ (accessed 24 January 2018).
[28] J.J. Spivey, Y.-F. Han, Catalysis (Specialist Periodical Reports: Volume 29), first edition, Royal Society of Chemistry, Croydon, 2017, pp. 265–281.
[29] V.I. Savchenko, I.A. Makaryan, Palladium catalyst for the production of pure margarine, Platinum Met. Rev. 43 (2) (1999) 74–82.
[30] G. Klauenberg, Hydrierung von Rüböl-Einfluß von Prozeßbedingungen und Produktqualitäten auf Verlauf und Ergebnis der Hydrierung, Eur. J. Lipid Sci. Technol. 86 (S1) (1984) 513–520.
[31] How to Calculate the True Cost of Steam, U.S. Department of Energy, Industrial Technologies Program-Energy Efficiency and Renewable Energy, Washington, DC, 2003.
[32] E.E.G. Rojas, J.S. Coimbra, J. Telis-Romero, Thermophysical properties of cotton, canola, sunflower and soybean oils as a function of temperature, Int. J. Food Prop. 16 (7) (2013) 1620–1629.
[33] U.S. Energy Information Administration Home Page-Natural Gas. https://www.eia.gov/naturalgas/ (Accessed 20 December 2017).
[34] K. Paffel, Steam Systems Best Practices Document No. 20, Swagelok Energy Advisors, Inc., Baton Rouge, LA, 2010.
[35] E.L. Paul, V.A. Atiemo-Obeng, S.M. Kresta, Handbook of Industrial Mixing: Science and Practice, John Wiley & Sons, Ltd., Inc., Hoboken, NJ, 2004, pp. 376–378.
[36] P.A. Ramachandran, R.V. Chaudhari, Three-Phase Catalytic Reactors, Gordon and Breach Science Publishers, London, 1983, pp. 285–298.
[37] B. Esteban, J.R. Riba, G. Baquero, A. Rius, R. Puig, Temperature dependence of density and viscosity of vegetable oils, Biomass Bioenergy 42 (2012) 164–171.
[38] H. Noureddini, B.C. Teoh, L.D. Clements, Viscosities of vegetable oils and fatty

acids, J. Am. Oil Chem. Soc. 69 (12) (1992) 1189–1191.
[39] M.J.F. Sánchez, Estudio de la utilización de catalizadores y reactores estructurados en la hidrogenación de aceites, Ph.D. Thesis, Universidad Nacional del Sur, Argentina, 2011 March.
[40] I. Hoek, Towards the catalytic application of a monolithic stirrer reactor. Ph.D. Thesis, Technische Universiteit Delft, The Netherlands, 2004 October.
[41] D.E. Boldrini, J.F. Sánchez Morales, G.M. Tonetto, D.E. Damiani, Monolithic stirrer reactor: performance in the partial hydrogenation of sunflower oil, Ind. Eng. Chem. Res. 51 (38) (2012) 12222–12232.
[42] P. Harriot, Chemical Reactor Design, Marcel Dekker, Inc., New York, NY, 2003, pp. 327–331.
[43] U.S. Energy Information Administration Home Page-Electricity. https://www.eia.gov/electricity/ (Accessed 20 December 2017).
[44] Evonik Industries Home Page-Catalyst Cost Calculation Tool. http://catalysts.evonik.com/product/catalysts/resources/CCCT.html (Accessed 22 January 2018).
[45] N. Fedotiev, S. Grilijes, Electropulido y Anodizado de Metales, Gustavo Gili, Barcelona, 1972, pp. 211–239.
[46] D.E. Boldrini, Desarrollo de catalizadores monolíticos con sustrato de aluminio anodizado, Ph.D. Thesis, Universidad Nacional del Sur, Argentina, 2015 March.
[47] G.F. Froment, K.B. Bischoff, Chemical Reactor Analysis and Design, second edition, John Wiley & Sons, Inc., New York, NY, 1990, pp. 367–373.
[48] A.F. Mills, Heat and Mass Transfer, Richard D, Irwin, Inc., Homewood, IL, 1995, pp. 705–806.
[49] I. Hoek, T.A. Nijhuis, A.I. Stankiewicz, J.A. Moulijn, Performance of the monolithic stirrer reactor: applicability in multi-phase processes, Chem. Eng. Sci. 59 (2004) 4975–4981.